A Field Study of Soil Biochar Treatment Response Using Small Unmanned Aerial Systems (sUAS)

Di An[1], Derek Hollenbeck[2], Si Gao[3], YangQuan Chen[1,2,*]
[1]Electrical Engineering & Computer Science, University of California, Merced
[2]Department of Mechanical Engineering, University of California, Merced
[3]Department of Life and Environmental Sciences, University of California, Merced
{dan7, dhollenbeck, sgao14, ychen53}@ucmerced.edu

***Abstract*—Biomass from agriculture production can be converted to biochar using the pyrolysis gasification process, which reduces the carbon footprint when added to soil. How to precisely, promptly, cost-effectively, and on a large scale map, the effect of biochar applied to soil in terms of water holding capacity continues to be a significant challenge. This paper is the first to reveal a comprehensive study demonstrating the feasibility of adding biochar to enhance the quantifying of soil temperature and soil moisture using image indexes (Visible Atmospherically Resistant Index (VARI) and Normalized Difference Vegetation Index (NDVI)). The significance of this work is that it provides the foundation for the subsequent assessments of carbon-negative technologies. We evaluated the correlation of VARI, NDVI, and soil temperature, Volumetric Water Content (VWC) under different treatments. Results show that the correlations of NDVI, VARI, and soil temperature and VWC in the treatment with biochar were 52.94% and 46.77% higher than those in the soil without biochar.**

***Index Terms*—Biochar, Remote Sensing, sUAS, NDVI, VARI, VWC**

I. Introduction

Biochar is a solid material generated during the pyrolysis of biomass. Biochar can be applied to soil to enhance soil functions and offset greenhouse gas emissions caused by biomass that would otherwise decay naturally into greenhouse gas (GHG). The benefits of biochar to soil fertility include the extraordinarily high binding affinity of nutrients for biochar and other molecules (adsorption), and the biochar's remarkable retention in the ground (stability) [1]. Additionally, sustained biochar application can generate oil and gas byproducts collected and used as fuel, resulting in clean, renewable energy and soil improvement. This is one of the negative emissions technologies (NETs) [2] that ensures that the final product becomes the real meaning of "carbon negative".

Unmanned aerial vehicles (UAVs) have been widely employed in agricultural applications as a novel remote sensing platform, including crop yield estimation [3], irrigation management [4], [5], and pest control [6], [7]. In comparison to satellites, UAVs may fly more freely and often in the field. The UAVs fly at a lower height and capture pictures of crops at a greater resolution [8]. Additionally, UAVs reduce the cost of data collecting compared with using other remote sensing methods such as satellite sensing.

In addition, one of our objectives of our field study is to reveal the relationship of affection between soil temperature and soil moisture with soil amendment (biochar). This investigation requires the ground truth data to map the temperature and moisture in the temporal and spatial domain, respectively. The UAV with the benefits we mentioned earlier is the great platform to implement our mission and would not be able to miss the growing season.

Previous research on soil temperature and moisture has concentrated chiefly on obtaining a soil sample and then analyzing it using a multimillion-dollar analyzer [9] to isolate the various components of soil [10]. Several researchers embedded carrierable devices on soil fields and inserted sensors in the soil to detect [11]. Additionally, a few studies employ remote sensing technology such as satellites and unmanned aerial systems (UAS) [12], [13] to assess soil conditions and carbon emissions (such as GHG). These prior attempts are mainly relied on the expensive analyzer and limited to the environment variable (which means cannot operate their analyzer or collect valid samples due to the rainy day, human activities, etc [14]). Some works using UAV and NDVI index to evaluate the growth, especially soil moisture, evapotranspiration, and their minor element contents [15]–[20]. However, these attempts didn't explain which level of soil moisture can be accurately predicted by NDVI, and also whether these image indexes can correlate with soil temperature for further explaining of carbon activities (such as GHG emissions). Therefore, we designed our field study with three benefits (innovations):

- The UAV equipped with thermal and near infrared (NIR) cameras helps us monitor the soil amendment effects on large-scale soil in real-time.
- Compared with the different depths of VWC with NDVI to find the better correlation.
- Introduced the VARI to build a relationship with soil temperature even if there are disturbances (green plants) in between.

As a result, we target two challenges in this paper: 1) what's the best sensing mechanism for using NDVI and VARI to

*Address all correspondence to this author.

reflect different depths of soil water content 2) what's the optimized fitting model of these indexes with soil temperature and moisture. The contributions of this work are as follows:

1) To the best of our knowledge, this is the first time study validating the optimized depth of VWC correlated by the NDVI.
2) After adding biochar amendment, we revealed a solid potential correlation between vegetation index and soil temperature.
3) We validated a field study in the winter growing season by conducting a series of intense sUAS flight and ground truth data collection.

II. Materials and Methods

A. Study Field Site and UASs Remote Sensing Configuration

We established a field experiment at a wheat (winter) rotational cropping system near the Philip Verwey Farm in Madera, CA (36.94° N, 120.378° W) in October 2021. The study site exhibits a Mediterranean climate with a mean annual temperature of 18.2°C and mean annual precipitation of 311mm. Summer is hot and dry (e.g., July average temperature is 29.3°C with an average precipitation of 0 mm) while winter is relatively cool and damp (e.g., January average temperature is 8.5°C with a 56 mm monthly average precipitation).

Biochar used in the field trial was the Rogue biochar produced by Oregon Biochar Solution (White City, OR, USA). The feedstock of biochar consisted of approximately 85% Douglas fir and ponderosa pine wood waste mixture, 14-15% almond and walnut tree pruning, and less than 1% of nutshells. Biochar particles had diameters ranging from 3 mm to 1 cm. Manure compost and biochar manure co-compost were prepared on-site at the Verwey farm during August - September 2021. Briefly, the manure-only pile consisted of approximately 15.34t of fresh solid manure and 1.32t of orchard clipping residues. The biochar co-compost pile consisted of 15.35t of fresh solid manure, 1.32t orchard clipping residues, and 1.0t of biochar.

Replicated treatment plots (2m x 12m with 2m buffer in between) were laid out in a randomized block design ($n = 4$) at our study site (Figure 1a). Treatments were applied to plots (a total of 16 plots) one week prior to seeding. All plots were seeded to winter wheat for the winter growing season on October 29th, 2021. The four treatments employed in this field trial were: 1) Control with no additional amendment; 2) Manure compost applied at 20 t/ha; 3) Biochar applied at 10 t/ha, and 4) Biochar manure co-compost applied at 17.5t/ha. All treatments were applied at equivalent C rates of 8 MgC/ha, see Figure 1b. Treatments were applied to the surface soil and incorporated to approximate 15cm depth with a rake and tines of a pitchfork. We also gently raked control plots to ensure consistency. A single time of flood irrigation was adopted following the landowners' common practices on November 11th, 2021. Our study site received no fertilizer input during the winter growing season, and the nutrient source for winter wheat was solely from the decomposition of crop residues left from the previous growing season.

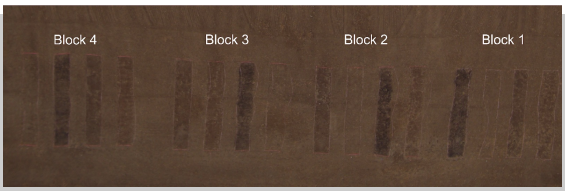

(a) Biochar plots locates at Verwey Farm

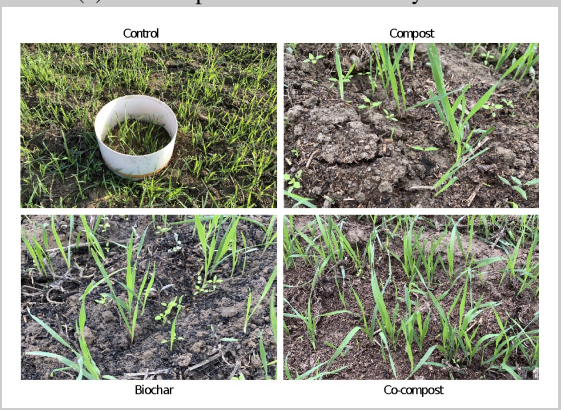

(b) Four treatments of soil and their plants growth

Fig. 1: (a) Replicated treatment plots (2 m x 12 m with a 2 m buffer) were laid out in a randomized block design in four blocks. biochar (10 t/ha), compost (20 t/ha), and co-compost (17.5 t/ha) were surface applied and incorporated. (b) Control, biochar, compost, and co-compost plots in one replicated block.

We employed a Hover quadcopter[1] as our UAV platform. A Pixhawk flying controller, GPS, and telemetry antenna were installed on the Hover. Additionally, it is capable of flying over a biochar treatment field utilizing the waypoints setting (designed by using Mission Planner software[2]). The Hover's lithium battery has a capacity of 9500 mAh, which is adequate for a 30-minute flight mission with the Hover's cameras mounted (this battery also powers the camera).

In this field study, multi-spectral images were collected by Survey 2 (MAPIR, USA)[3]cameras with 4 bands, blue, green, red (RGB), and near-infrared (NIR). The MAPIR camera has a resolution of 4608 x 3456 pixels and a spatial resolution of 1.01 cm/pixel. Besides, thermal images of the biochar treatment field were collected using the ICI 9640 P-Series thermal camera (ICI, USA). The thermal camera has a 640 x 480 pixel resolution. The precision was expected to be 1°C. The thermal camera will verify whether the soil temperature can be measured through different treatments and plants. Furthermore, the flight height of the three cameras was settled at 30m, 30m, and 40m, respectively. The overlap of Field of View (FOV) was adjusted to 75% for all aircraft missions to ensure that the photos could be stitched together during image pre-processing. From late October 2021 to early February 2022, we did the flight mission biweekly on our biochar

[1]https://www.foxtechfpv.com/foxtech-hover-1-quadcopter.html
[2]https://ardupilot.org/planner/
[3]https://www.mapir.camera/collections/survey2

treatment field. All cameras' reflectance was calibrated before the flight by using a color panel.

B. Geospatial Interpolation with Kriging

In geostatistics, one of the common problems encountered is to spatially interpret and estimate a set of unknown data locations, $z(s_0)$, from a set of sparse observations, $z(s_i)$, at locations s_0 and s_i, respectively. These N sparse sampling points, are taken inside a domain $\Omega \in \mathbb{R}^2$ and aim to find a set of weights, λ_i, to estimate the value at the unknown locations,

$$\hat{z}(s_0) = \sum_{i=1}^{N} \lambda_i z(s_i). \tag{1}$$

For ordinary kriging [21], a semivariogram is used to represent the spatial variability. For a given spatial distance between observations, h, the point support semivariogram is written as,

$$\hat{\gamma}(h) = \frac{1}{2N(h)} \sum_{i=1}^{N(h)} (z(s_i) - z(s_i + h))^2, \tag{2}$$

such that $N(h)$ is the number of observartions with distance of h. Using this experimental semivariogram data (2) a semivariogram model is typically fit using one of the several common functions (circular, spherical, exponential, Gaussian, or linear). Finally, given the semivariogram model, the kriging weights can be determined by solving the linear system,

$$\sum_{j=1}^{N} \lambda_j C(\mathbf{s}_i - \mathbf{s}_j) + \mu(\mathbf{s}_0) = C(\mathbf{s}_i - \mathbf{s}_0), \text{ for } i = 1, 2, ..N, \tag{3}$$

where $C(\cdot)$ represents the point support covariance matrix. This covariance matrix has an important relationship to the semivariogram, such that, $\gamma(h) = C(0) - C(h)$ [21]. The estimation error variance is shown to be $\sigma_e^2 = Var(z(s_0) - \hat{z}(s_0))$, which for ordinary kriging, is minimized to make the estimated values $\hat{z}(s_0)$ optimal. In order for the estimator to be unbiased (e.g. $E[\hat{z}(s_0)] = E[z(s_0)]$), kriging requires $\sum \lambda_i = 1$ and the spatial mean to be stationary $E[z(s)] = \mu, \ \forall s \in \Omega$.

In this work we utilize kriging with the ground truth temperature measurements to compare with TIR imagery and ice water calibration. The workflow is illustrated in Fig. 2.

C. Statistical Analysis

We decided to use The VARI and NDVI are used to verify whether these two indexes can indicate the soil temperature and its moisture at different treatments based on multiple-spectral images collected. The default equation to generate these indexes are as referred (4) and (5), respectively.

$$\texttt{VARI} = \frac{\texttt{Green} - \texttt{Red}}{\texttt{Green} + \texttt{Red} - \texttt{Blue}} \tag{4}$$

$$\texttt{NDVI} = \frac{\texttt{NIR} - \texttt{Red}}{\texttt{NIR} + \texttt{Red}} \tag{5}$$

The VARI method is a vegetation index that enables a quantitative estimate of vegetation proportions using only visible light. In other words, this index highlights the green vegetation

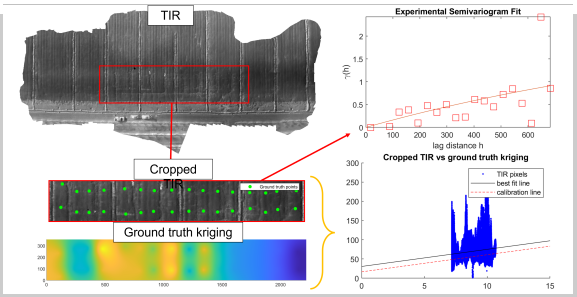

Fig. 2: The TIR imagery is cropped in this diagram to enclose only the biochar plots. The geolocations of the ground truth measurements are identified and used to fit an experimental exponential semivariogram with a lag of 700 pixels. The resulting semivariogram is used to krige the ground truth measurements to match the TIR imagery size. Lastly, the pixel by pixel correlation plot between the cropped TIR image and ground truth kriging is constructed with the best fit line. This best fit line's y-intercept is then corrected using the pixel intensity and a known temperature ice bath.

on the ground to make the soil, rocks, and plants clearly distinguishable. The NDVI method is a standardized index that permits the construction of a visual representation of the degree of greenness in a given area (relative biomass). This index uses the contrast between chlorophyll pigment absorptions in the red band and the high reflectivity of plant components in the near-infrared region of a multispectral dataset. This index returns values in the range of [-1.0, 1.0] [22].

To illustrate the variety of different treatments, we would plot all the data and use a linear regression model to seek the relationship between the index, soil temperature, and VWC at different depths of soil. The R^2 and standard deviation (STD) would be used to evaluate the strength of the relationship between soil temperature, VWC and image indexes.

III. Experiments and Results

We scheduled our flight missions bi-weekly during the winter growing season. Every time we captured RGB, NIR, and thermal information from the ground, the ground truth data such as soil temperature and VWC would also be collected by thermometer and soil suction lysimeter [4]. The scatter would be first to plot to observe their potential trends relationship between these information. We extracted two points (Kriging, see details in section II-B) of VARI and NDVI values from our total plots individually. Please see details in the following sections.

A. Correlation analysis of the VARI and NDVI indexes versus temperature

In general, the soil temperature in November is higher than in January. The temperature in the middle of California was still suffering from the dry season, and the farmers had just seeded the wheat in the early part of November, which meant the soil was exposed to sunlight, and there were no green plants on the ground. From Figure 8a, we can see that the average R^2 is the maximum ($R^2 = 0.5$), and its dispersion is

[4] https://www.hannainst.com/suction-lysimeter-for-root-level-soil-monitoring.html

the minimum ($STD = 0.19$), which indicates the VARI index has the potential ability to predict the soil temperature within biochar amendment.

The NDVI has a weaker indicating ability than VARI for the soil temperature. However, the plots of adding biochar amendment still have the most significant difference in R^2 and STD, which also verified that NDVI has the remarkable ability to predict the temperature better than the other treatment blocks.

Overall, the VARI and NDVI can both reveal the soil temperature. Biochar as an amendment would help quantify the soil temperature and VWC based on UAV sensing. The average enhanced correlation rate of VARI from biochar treatment is 46.77%, compared with control, manure, and mixture treatments. Relative to the mixture treatment, the NDVI from biochar treatment enhanced the correlation rate was 52.94%.

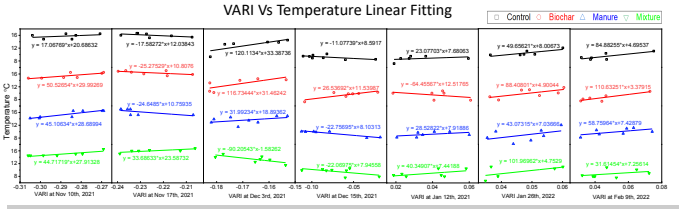

Fig. 3: VARI Vs Temperature. The x-axis indicates the VARI and NDVI values, and the y-axis indicates the ground truth of soil temperature, The dark, red, blue, and green lines are represented by control, biochar, manure, and mixture treatments, respectively.

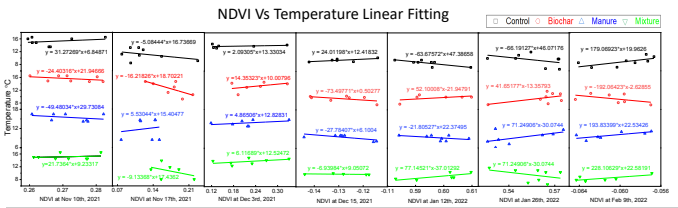

Fig. 4: NDVI Vs Temperature. The x-axis indicates the VARI and NDVI values, and the y-axis indicates the ground truth of soil temperature, The dark, red, blue, and green lines are represented by control, biochar, manure, and mixture treatments, respectively.

B. Correlation analysis of the NDVI index versus different depths of VWC

As we all know, biochar has strong water retention ability [1]. However, quantifying the biochar water retention ability on a large scale is still a challenge. Fortunately, the soil moisture can be indicated by the health and growth of the biomass (NDVI). Therefore, we compared different depths of VWC with NDVI values, see Figures 5, 6, and 7.

In Figure 8b, the correlation of NDVI and VWC at 7.5 cm is the most significant. Even if the control treatment has the maximum difference in STD and averages R^2, the biochar treatment has the minimum STD and is not too low in R^2. We believe the most reliable method is essential to improve the quantifying accuracy by using NDVI. In Figure 5 and Figure 6. The average VWC from biochar treatments is higher than the other treatment plots, which verifies that biochar could enhance water conservation and crop productivity. As of Figure 7, there is barely any relationship in these different treatments where VWC is at 15cm.

IV. Discussion and Challenges

At Nov 17th, we can see the fitting lines of treatments are pretty short (Figure 4). Based on our literature review, biochar can reflect the near-infrared wave [23], this mechanism may affect the reflectance of biochar and natural green plants. However, how it affects the reflectance of the biochar, mixture, and green plants needs more exploration in the future.

In November, the VWC is much higher than the rest of the month due to farmers did flood irrigation once on the whole field. Although wheat growth is related to soil water content, correlation directions are different where VWC is at 4 cm and 7.5 cm. All biochar treatments have a positive correlation with VWC at 4 cm. However, the correlations of VWC at 7.5cm are various. This would also need to be further explored.

In the future, we will provide further statistic analysis for our proposed regression model. We would plan to train the comprehensive model as well to fit these indexes with soil temperature and moisture so that we can use these indexes to explain soil carbon activities, such as methane and CO_2 emissions. We believe an effective method of quantifying carbon emissions still needs to be explored.

V. Conclusions

In this paper, we validated a field study in which UAVs were used to check on the soil for a whole growing season after biochar was added as a soil amendment. The relationship revealed between soil temperature and volume water content is able to be described by linear regression models. After applying different treatments, we illustrated that the soil temperature and VWC can still be reflected by the VARI and NDVI indexes. The addition of biochar as a soil amendment would enhance the sensing accuracy, and the correlation rate using VARI is about 46.77% higher than the non-treatment plots, and the NDVI index is 52.94% higher than the other treatments. The NDVI has a comprehensive prediction where VWC will be measured at 7.5cm. All in all, our results show that image index analysis has a lot of potential to become a fast way to measure the condition of soil by adding biochar.

Acknowledgment

We wish to thank Brendan Harrison, Melinda Gonzales, and Touyee Thao for sampling field trials ground-truth data. Thanks Haoyu Niu for flight mission help. This work is partly supported by SGC project[5] entitled “Mobile Biochar Production for Methane Emission Reduction and Soil Amendment.” Grant Agreement #CCR20014.

[5]https://mechatronics.ucmerced.edu/mobilebiochar

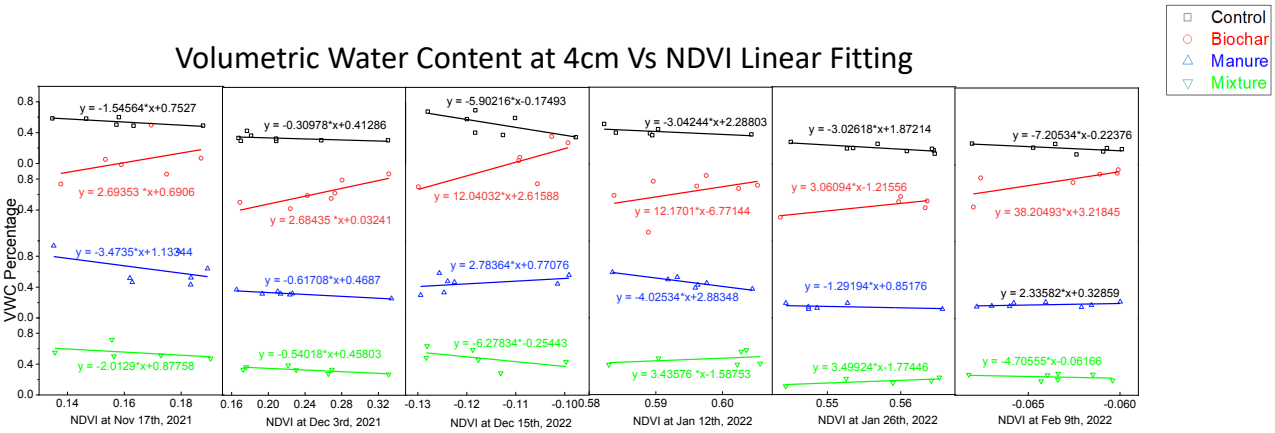

Fig. 5: VWC at 4cm. The x-axis is represented as the NDVI value, and the y-axis is represented as the VWC (range from 0 to 2. VWC > 1 means water is greater than soil in the same unit, same unit of y-axis for the rest of the VWC figures

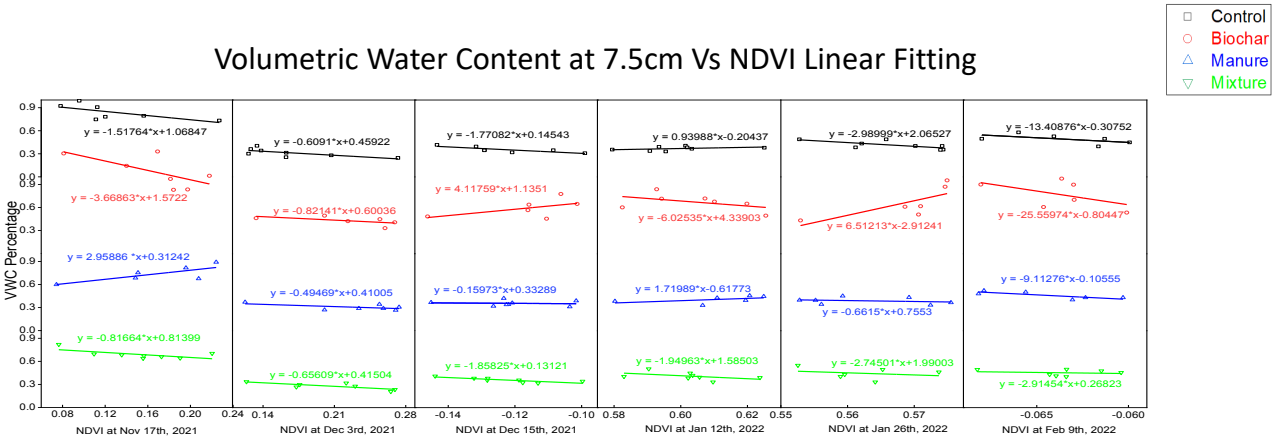

Fig. 6: VWC at 7.5cm. The x-axis is represented as the NDVI value, and the y-axis is represented as the VWC

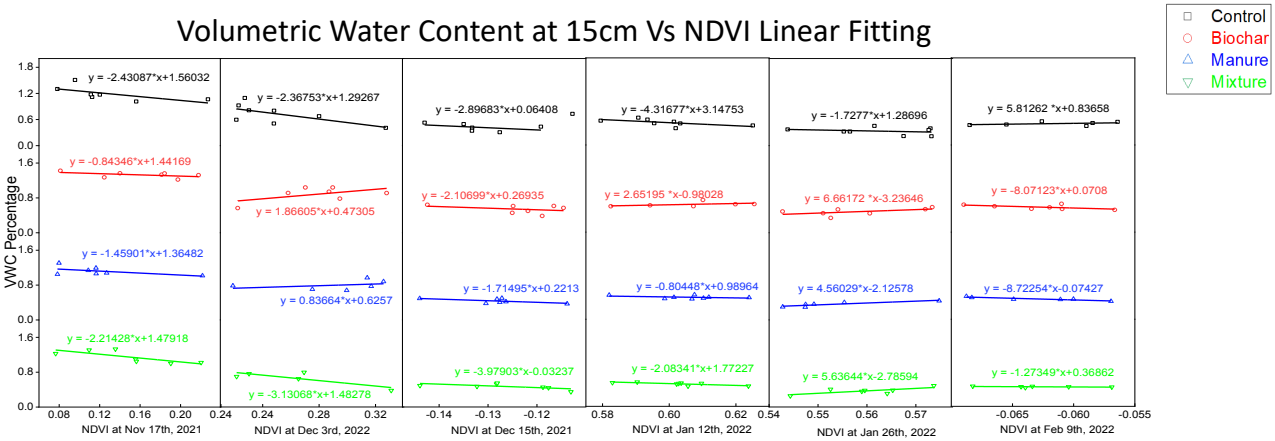

Fig. 7: VWC at 15cm. The x-axis is represented as the NDVI value, and the y-axis is represented as the VWC

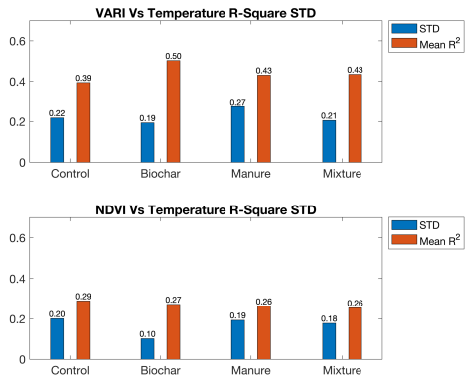

(a) The R^2 of VARI and NDVI versus temperature

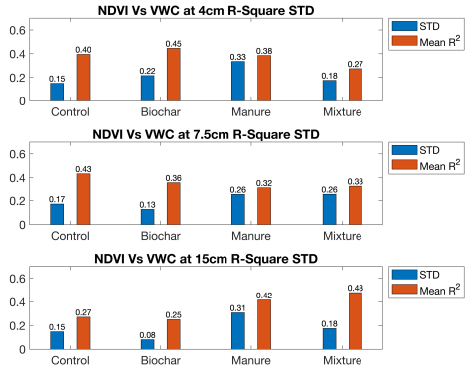

(b) The R^2 of VWC versus NDVI at different depth level

Fig. 8: a) The R^2 and STD for the VARI and NDVI versus soil temperature. b) The R^2 and STD of NDVI versus three different depths of the VWC.

REFERENCES

[1] D. An, H. Niu, and Y. Chen, "A Non-intrusive quantification method for biochar water retention capacity using a portable microwave sensor and machine learning," in *Proceedings of 2021 9th International Conference on Control, Mechatronics and Automation (ICCMA)*. IEEE, 2021, pp. 152–157.

[2] K. Anderson and G. Peters, "The trouble with negative emissions," *Science*, vol. 354, no. 6309, pp. 182–183, 2016.

[3] T. Zhao, Z. Wang, Q. Yang, and Y. Chen, "Melon yield prediction using small unmanned aerial vehicles," in *Proceedings of Autonomous Air and Ground Sensing Systems for Agricultural Optimization and Phenotyping II*, vol. 10218. SPIE, 2017, pp. 53–58.

[4] T. Zhao, A. Koumis, H. Niu, D. Wang, and Y. Chen, "Onion irrigation treatment inference using a low-cost hyperspectral scanner," in *Proceedings of Multispectral, Hyperspectral, and Ultraspectral Remote Sensing Technology, Techniques and Applications VII*, vol. 10780. International Society for Optics and Photonics, 2018, p. 107800D.

[5] H. Niu, T. Zhao, D. Wang, and Y. Chen, "A UAV resolution and waveband aware path planning for onion irrigation treatments inference," in *Proceedings of 2019 International Conference on Unmanned Aircraft Systems (ICUAS)*. IEEE, 2019, pp. 808–812.

[6] R. Näsi, E. Honkavaara, P. Lyytikäinen-Saarenmaa, M. Blomqvist, P. Litkey, T. Hakala, N. Viljanen, T. Kantola, T. Tanhuanpää, and M. Holopainen, "Using UAV-based photogrammetry and hyperspectral imaging for mapping bark beetle damage at tree-level," *Remote Sensing*, vol. 7, no. 11, pp. 15 467–15 493, 2015.

[7] H. Niu, T. Zhao, and Y. Chen, "Intelligent bugs mapping and wiping (iBMW): An affordable robot-driven robot for farmers," in *Proceedings of 2019 IEEE International Conference on Mechatronics and Automation (ICMA)*. IEEE, 2019, pp. 397–402.

[8] T. Zhao, H. Niu, A. Anderson, Y. Chen, and J. Viers, "A detailed study on accuracy of uncooled thermal cameras by exploring the data collection workflow," in *Proceedings of Autonomous Air and Ground Sensing Systems for Agricultural Optimization and Phenotyping III*, vol. 10664. SPIE, 2018, pp. 105–112.

[9] J. Aníbal, C. Veiga-Pires, and E. Esteves, "Effects of spoilage on nitrogen and carbon stable isotopes signatures of the clam," in *INCREASE: Proceedings of the 1st International Congress on Engineering and Sustainability in the XXI Century-INCREASE 2017*. Springer, 2018, p. 241.

[10] P. Rochette, L. Flanagan, and E. Gregorich, "Separating soil respiration into plant and soil components using analyses of the natural abundance of carbon-13," *Soil Science Society of America Journal*, vol. 63, no. 5, pp. 1207–1213, 1999.

[11] M. Hanada, H. Koda, K. Onaga, K. Tanaka, T. Okabayashi, T. Itoh, and H. Miyazaki, "Portable oral malodor analyzer using highly sensitive in2o3 gas sensor combined with a simple gas chromatography system," *Analytica Chimica Acta*, vol. 475, no. 1-2, pp. 27–35, 2003.

[12] D. An and Y. Chen, "Application of smart, swarm and small UAV's for methane emission reduction," in *Proceedings of International Design Engineering Technical Conferences and Computers and Information in Engineering Conference*, vol. 85437. American Society of Mechanical Engineers, 2021, p. V007T07A050.

[13] ——, "Digital Twin enabled methane emission abatement using networked mobile sensing and mobile actuation," in *Proceedings of 2021 IEEE 1st International Conference on Digital Twins and Parallel Intelligence (DTPI)*, 2021, pp. 354–357.

[14] J. Green, J. Likar, and Y. Shprits, "Impact of space weather on the satellite industry," *Space Weather*, vol. 15, no. 6, pp. 804–818, 2017.

[15] R. Heidarian Dehkordi, H. Pelgrum, and J. Meersmans, "High spatio-temporal monitoring of century-old biochar effects on evapotranspiration through the ETLook model: a case study with uav and satellite image fusion based on additive wavelet transform (AWT)," *GIScience & Remote Sensing*, vol. 59, no. 1, pp. 111–141, 2022.

[16] I. Zafeiriou, D. Gasparatos, D. Ioannou, D. Kalderis, and I. Massas, "Selenium biofortification of lettuce plants (lactuca sativa l.) as affected by Se Species, Se Rate, and a Biochar co-application in a Calcareous soil," *Agronomy*, vol. 12, no. 1, p. 131, 2022.

[17] Á. Horel and E. Tóth, "Changes in the soil–plant–water system due to biochar amendment," *Water*, vol. 13, no. 9, p. 1216, 2021.

[18] H. Jin, C. J. Köppl, B. M. Fischer, J. Rojas-Conejo, M. S. Johnson, L. Morillas, S. W. Lyon, A. M. Durán-Quesada, A. Suárez-Serrano, S. Manzoni *et al.*, "Drone-based hyperspectral and thermal imagery for quantifying upland rice growth and water use efficiency after biochar application," 2021.

[19] R. Heidarian Dehkordi, V. Burgeon, J. Fouche, E. Placencia Gomez, J.-T. Cornelis, F. Nguyen, A. Denis, and J. Meersmans, "Using UAV collected RGB and multispectral images to evaluate winter wheat performance across a site characterized by century-old biochar patches in Belgium," *Remote Sensing*, vol. 12, no. 15, p. 2504, 2020.

[20] C. Nzediegwu, S. Prasher, E. Elsayed, J. Dhiman, A. Mawof, and R. Patel, "Effect of biochar on the yield of potatoes cultivated under wastewater irrigation for two seasons," *Journal of Soil Science and Plant Nutrition*, vol. 19, no. 4, pp. 865–877, 2019.

[21] H. Wackernagel, "Ordinary kriging," in *Multivariate Geostatistics*. Springer, 2003, pp. 79–88.

[22] A. A. Gitelson, Y. J. Kaufman, R. Stark, and D. Rundquist, "Novel algorithms for remote estimation of vegetation fraction," *Remote Sensing of Environment*, vol. 80, no. 1, pp. 76–87, 2002.

[23] J. B. Reeves, P. Falcao, and N. Comerford, "Spectral effects of biochar on NIR and mid-IR spectra of soil/char mixtures," in *Proceedings of the 19th World Congress of Soil Science, Soil Solutions for A Changing World*, 2010.